

IR detection using type-II superlattice photodiodes

T2SL (Type II SuperLattice) or sometimes also called SLS (Strained Layer Superlattice) is a material / technology that can be used to make high quality cooled infrared photon detectors with a cut-off wavelength ranging from 2 μm to 30 μm . This covers the SWIR, MWIR, LWIR and VLWIR wavelength bands, loosely defined as 2-3 μm , 3-5 μm , 8-12 μm and $>12 \mu\text{m}$, respectively.

A superlattice is a system made of a repeating sequence of thin layers of different materials. If the layer thicknesses are small enough in a quantum mechanical sense, minibands are formed in the material. The result is an artificial material with properties that can be engineered; in the detector case the bandgap energy corresponding to the desired cut-off wavelength. When two semiconductors are brought in contact, there are several ways the valance and conduction bands can align. If both the valance and the conduction band edge of the second material are above the band edges of the first material, it is called a broken type II band alignment.

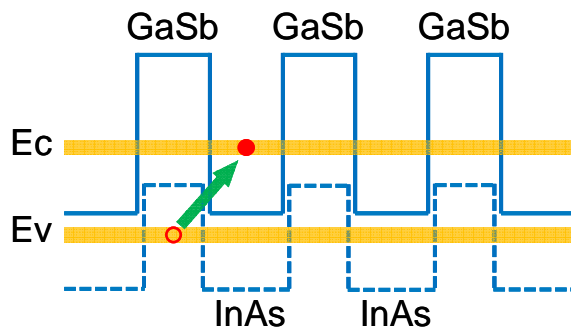


Figure 1 Band alignment of InAs GaSb and the forming of minibands.

The III/V compound materials InAs and GaSb form such a band alignment (see Figure 1). As can be seen in Figure 2, InAs has a lattice mismatch of less than 1% on GaSb. Starting with GaSb substrates alternating layers of InAs and GaSb with atomic layer precision can be deposited using MBE (Molecular Beam Epitaxy). By interface engineering (create an interface layer of InSb) or using more complicated superlattices like $\text{Ga}_x\text{In}_{1-x}\text{Sb}/\text{InAs}$, thick strain compensated structures with high crystal quality can be grown. If doping in the form of trace amounts of Be, Te or Si is incorporated, photovoltaic p-i-n structures that can be used to detect IR radiation of the desired wavelength are formed.

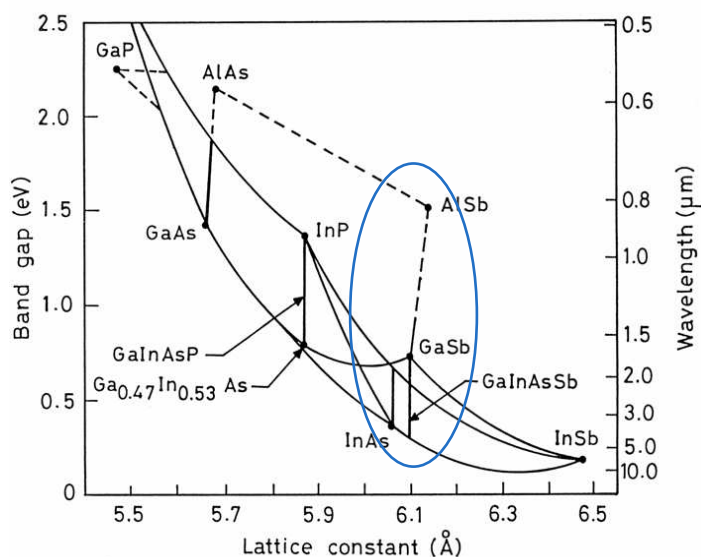


Figure 2 Lattice constants and band gap energy of several III/V materials

Surface currents have historically been the limiting factor, but recently this weakness has been overcome by dielectric passivation.^{1,2}

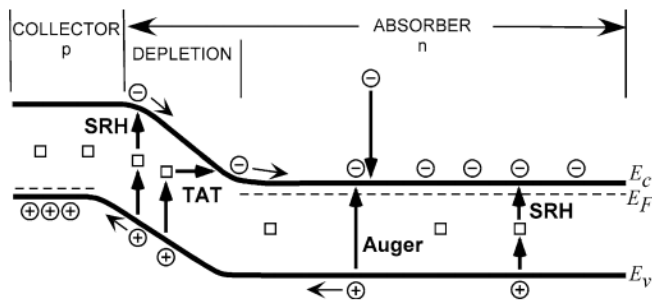


Figure 3. Dark current generation mechanisms in an infrared photodiode. SRH = Shockley-Read-Hall generation; TAT = trap assisted tunneling (or thermally assisted tunneling). This figure is taken from ref. 3.

Figure 3 shows the three major dark current mechanisms in infrared photodiodes at typical operating temperatures and bias. Of these, the Auger generation process dominates in mercury-cadmium-telluride (MCT) detectors. Dark current from this process is generated throughout the entire volume of material with free carriers. This includes the absorber and contact layers, but not the depletion region. To first order, it is therefore a bias-independent current – a so-called “diffusion current”. The higher the doping, the larger is the Auger generation rate and common wisdom in MCT diode design is therefore to use very low background *p*-type or *n*-type doping in the absorber material to minimize the dark current.

Comparison with MCT

Rule 07 is a heuristic model which predicts dark current in state-of-the-art MCT devices as a function of cut-off wavelength and operating temperature. The underlying assumption is that the dark current is diffusion limited and has an activation energy close to that of the optical band gap of the absorber material. Furthermore, the absorber is assumed to be sufficiently thick to give 60% external quantum efficiency (QE) or better.

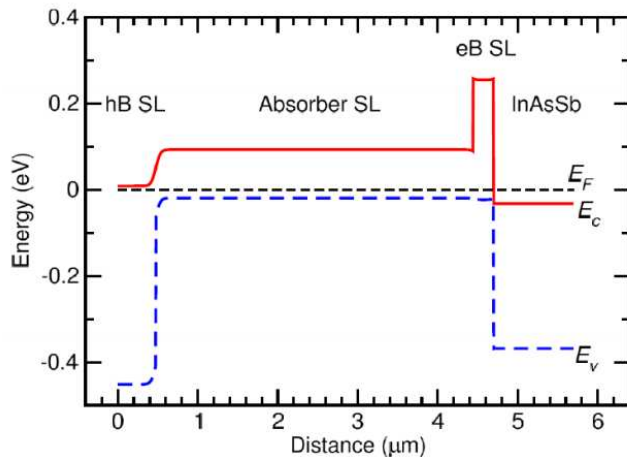


Figure 4 Complementary barrier infrared detector (CBIRD) with hole and electron barriers. The advantage of this and similar designs is that the depletion region of the *p*-*n* junction is located in material with higher bandgap, leading to lower SRH current generation.

Due to the strain of the individual layers in T2SL detectors the valence band structure is very different from that of MCT, and Auger processes are strongly suppressed. Instead, Shockley-Read-Hall (SRH) generation via mid-gap defects is the limiting process, with minority carrier lifetimes around 30 ns. These defects notwithstanding, with unipolar barriers and clever doping schemes^{3,4,5,6,7,8} (see, e.g. Figure 4) the dark current of state-of-the-art T2SL detectors is within a factor of 10 of that for the best MCT detectors with corresponding cut-off wavelength; see Figure 5. Should the mid-gap defects be reduced or passivated enough to render microsecond long SRH lifetimes, the expected dark current performance would far surpass that of MCT; see Figure 6.

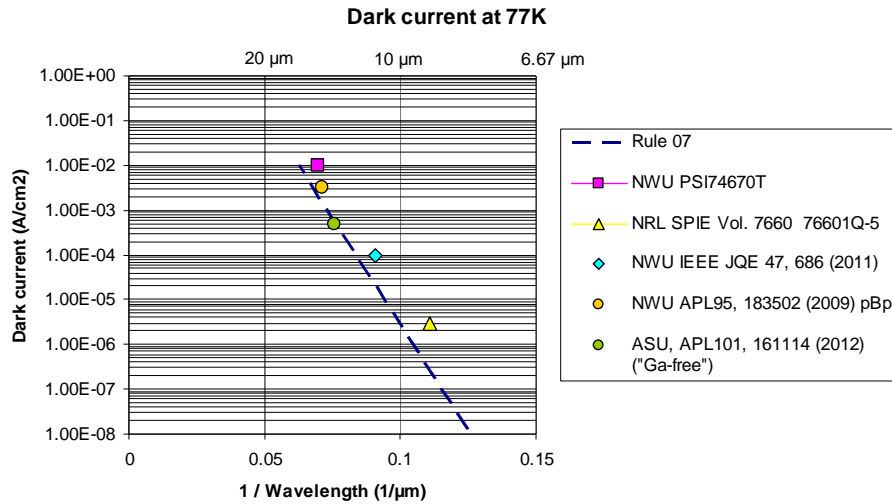


Figure 5 Dark current comparison of LWIR and VLWIR T2SL detectors against Rule07. NWU = Northwestern University [5,6,7]; NRL = Naval Research Labs [8]; ASU = Arizona State University [4]. The “Ga-free” entry is for an nBn device employing a 2.2 μm thick absorber of InAs/InAsSb T2SL grown on GaSb substrate. However, it should be noted that the responsivity is very low for this device, with a quantum efficiency of only 2.5%.

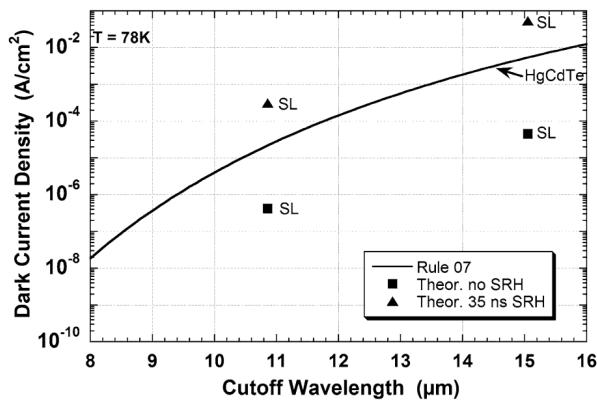


Figure 6 Theoretical dark current density for T2SL with 35 ns SRH lifetime and 1 μs SRH lifetime, as compared to Rule 07 for MCT. This figure is taken from ref. 3.

Quantum efficiency for T2SL detectors can be comparable with that of MCT for enough thick absorber layers: 50% or more is routinely obtained for absorber layers thicker than 3 μm.

The main disadvantage of MCT for long and very long wave IR (LWIR and VLWIR, respectively) is the extreme sensitivity of bandgap to composition; for $\text{Hg}_{1-x}\text{Cd}_x\text{Te}$ with $x = 0.20$ the bandgap at 80K is ~ 0.086 eV (14.4 μm), whereas for $x = 0.15$ the bandgap is zero (semimetal, infinite cutoff wavelength); see Figure 7. This makes uniformity over large areas difficult and expensive to achieve. In contrast, with T2SL the layers are binary compounds – no composition control necessary – and the cutoff wavelength is determined by the layer thicknesses alone. Since spatial uniformity of deposition rate in MBE equipment is dictated by simple geometric principles and chamber size this doesn't pose a problem. Indeed, as ref. [7] shows, excellent response and dark current uniformity is achieved for MBE-grown T2SL LWIR detectors over entire 75 mm dia. wafers.

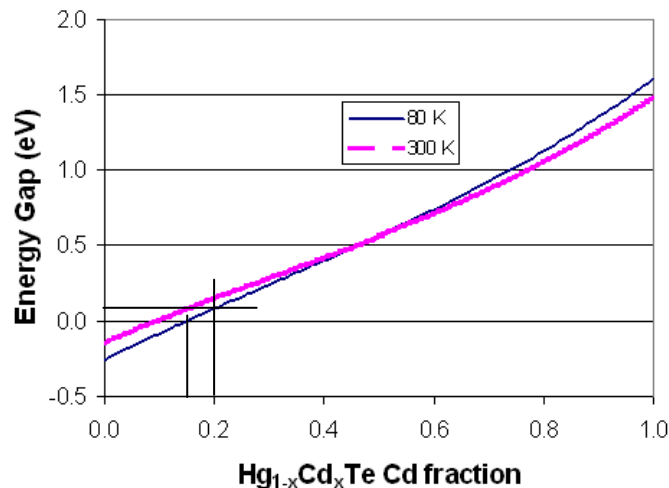


Figure 7 Bandgap of MCT versus the CdTe fraction x . Two vertical lines denote the compositions for $14.4 \mu\text{m}$ and infinite cutoff wavelength, respectively.

T2SL - State of the art

Some groups have already reported results on T2SL based SWIR detectors with cutoff around $2.5 \mu\text{m}$. Ref. [9] for instance demonstrates 320×256 imaging at room temperature with a FPA grown on InP and a dark current one order of magnitude smaller than MCT. Even more recent results¹⁰ based on InAs/GaSb/AlSb photodiodes grown on GaSb substrate show a high detectivity of 1.7×10^{10} Jones at room temperature and a quantum efficiency of 41.5%.

Dual-band MWIR/MWIR back-to-back photodiode FPA modules are currently in series production at AIM Infrarot-Module and Fraunhofer IAF, Germany, for an airborne military system. While representing a formidable technical task in many ways, this application does however not require high operating temperature, and will probably not push the technology's limits in that direction.

Recently reported MWIR FPA results prove that NETD < 20 mK is possible for $f/2.3$ optics at temperatures up to 120 K.¹¹ Furthermore, the BLIP temperature (defined for 2π FOV, 100% QE, 300 K) is as high as 180 K. This is not far from the BLIP temperature of state-of-the-art MCT material.¹²

In the LWIR range a $1\text{k} \times 1\text{k}$ focal plane array with 50% cutoff at $11 \mu\text{m}$ has been demonstrated. Impressively enough, a NETD below < 24 mK was reported for operating temperatures up to 81 K, an integration time of 0.13 ms and rather narrow $f/4$ optics. It was stressed by the authors that the spatial uniformity and homogeneity over the entire $3''$ epi wafer was excellent.¹³

Even dual band LWIR/LWIR FPA detectors have very recently been fabricated with very good results.¹⁴

¹ Pierre-Yves Delaunay, Andrew Hood, Binh Minh Nguyen, Darin Hoffman, Yajun Wei, and Manijeh Razeghi, "Passivation of type-II InAs/GaSb double heterostructure", Appl. Phys. Lett 91, 091112 (2007)

² R Chaghi, C Cervera, H Ait-Kaci, P Grech, J B Rodriguez and P Christol, "Wet etching and chemical polishing of InAs/GaSb superlattice photodiodes", Semicond. Sci. Technol. 24, 065010 (2009)

³ D. Rhiger, "Performance Comparison of Long-Wavelength Infrared Type II Superlattice Devices with HgCdTe", J. Electron. Mat. 40, 1815 (2011)

⁴ H. S. Kim et al., "Long-wave infrared nBn photodetectors based on InAs/InAsSb type-II superlattices", Appl. Phys. Lett. 101, 161114 (2012)

⁵ B.-M. Nguyen, S. Bogdanov, S. Abdollahi Pour, and M. Razeghi, "Minority electron unipolar photodetectors based on type II InAs/GaSb/AlSb superlattices for very long wavelength infrared detection", Appl. Phys. Lett. 95, 183502 (2009)

⁶ Manijeh Razeghi, Binh-Minh Nguyen, Pierre-Yves Delaunay, Edward Kwei-wei Huang, Siamak Abdollahi Pour, Paritosh Manukar, Simeon Bogdanov", State-of-the-art Type II Antimonide-based superlattice photodiodes for infrared detection and imaging", Proc. of SPIE 7467, 74670T (2009)

⁷ "Growth and Characterization of Long-Wavelength Infrared Type-II Superlattice Photodiodes on a 3-in GaSb Wafer", IEEE J. Quantum Electron. 47, 686 (2011)

- ⁸ E. H. Aifer, S. I. Maximenko, M. K. Yakes, C. Yi, C. L. Canedy, I. Vurgaftman, E. M. Jackson, J. A. Nolde, C. A. Affouda, M. Gonzalez, J. R. Meyer, K. P. Clark, P. R. Pinsukanjana, "Recent developments in type-II superlattice-based infrared detectors", Proc. of SPIE 7660, 76601Q (2010)
- ⁹ H. Inada, K. Miura, H. Mori, Y. Nagai, Y. Iguchi, Y. Kawamura, "Uncooled SWIR InGaAs/GaAsSb type II quantum wells focal plane array", Proc. of SPIE Vol. 7660, 76603N-1 (2010)
- ¹⁰ A.M. Hoang, G. Chen, A. Haddadi, S. Abdollahi Pour, M. Razeghi, "Demonstration of short wavelength infrared photodiodes based on type-II InAs/GaSb/AlSb superlattices", Appl. Phys. Lett. 100, 21101 (2012)
- ¹¹ S. Abdollahi Pour, E. K. Huang, G. Chen, A. Haddadi, B.-M. Nguyen, and M. Razeghi, "High operating temperature midwave infrared photodiodes and focal plane arrays based on type-II InAs/GaSb superlattices", Appl. Phys. Lett. 98, 143501 (2011)
- ¹² W.E. Tennant, "Rule 07' Revisited: Still a Good Heuristic Predictor of p/n HgCdTe Photodiode Performance?", J. Electron. Mat. 39, pp. 1030-1035 (2010) – using the dark current model in this paper, a similarly defined BLIP temperature of 200-210K is obtained for state-of-the-art MCT.
- ¹³ Paritosh Manurkar, Shaban Ramezani-Darvish, Binh-Minh Nguyen, Manijeh Razeghi, and John Hubbs, "High performance long wavelength infrared mega-pixel focal plane array based on type-II superlattices", Appl. Phys. Lett. 97, 193505 (2010)
- ¹⁴ Edward Kwei-wei Huang, Abbas Haddadi, Guanxi Chen, Binh-Minh Nguyen, Minh-Anh Hoang, Ryan McClintock, Mark Stegall, and Manijeh Razeghi, "Type-II superlattice dual-band LWIR imager with M-barrier and Fabry-Perot resonance", OPTICS LETTERS 36, 2560 (2011)